Journal of Organometallic Chemistry, 359 (1989) 371–378
Elsevier Sequoia S.A., Lausanne – Printed in The Netherlands

Organometallic macrocyclic complexes: the synthesis, electrochemistry and single crystal X-ray structure of $[Fe(C_5H_5)(L)]^+$ (L = 1,4,7-trithiacyclononane)

Alexander J. Blake, Rhona D. Crofts, Gillian Reid and Martin Schröder *

Department of Chemistry, University of Edinburgh, West Mains Road, Edinburgh EH9 3JJ (Scotland)

(Received May 27th, 1988)

Abstract

Reaction of $[Fe(C_5H_5)I(CO)_2]$ with one molar equivalent of L (L = 1,4,7-trithiacyclononane) affords the complex cation $[Fe(C_5H_5)(L)]^+$ in high yield. Crystals of $[Fe(C_5H_5)(L)]BPh_4$ are monoclinic, space group $P2_1/c$, with a 15.0461(14), b 10.5866(12), c 19.8032(18) Å, β 100.205(9)°, V 3104.48 Å^3, D_c 1.327 g cm^{-3}, $Z = 4$. The single crystal X-ray structure of the complex shows octahedral Fe^{II} with the carbocyclic and macrocyclic ligands bound facially to the metal centre, Fe–S(1) 2.2100(18), Fe–S(4) 2.2053(19), Fe–S(7) 2.2078(19), Fe–C 2.007(12)–2.112(12) Å. Two orientations of the C_5H_5 ring are observed. $[Fe(C_5H_5)(L)]PF_6$ shows a reversible one-electron $Fe^{II/III}$ couple at $E_{1/2} = +0.44$ V vs. Fc/Fc$^+$ in CH_3CN at platinum electrodes. Coulometry confirms that the oxidation is a one-electron process. The Fe^{III} complex has been characterised by ESR and UV-visible spectroscopy.

Introduction

Coordination complexes of thioether macrocyclic ligands are the subject of particular current interest in view of their unusual stereochemical, electronic and redox properties [1–7]. We are particularly interested in developing the coordination chemistry of small ring tridentate macrocycles, such as 1,4,7-trithiacyclononane (L), 1,4,7-triazacyclononane and 1,4,7-trimethyl-1,4,7-triazacyclononane towards the synthesis of redox-active piano-stool complexes of the type $[M(L)(X)(Y)(Z)]^{x+}$ (X,Y,Z = neutral or anionic ligands) [1]. As a start to this study, we report herein the synthesis, structure and electrochemistry of the mixed-sandwich complex cation $[Fe(C_5H_5)(L)]^+$.

To date the only reported Fe complexes of 1,4,7-trithiacyclononane (L) are the bis-sandwich species $[Fe(L)_2]^{2+/3+}$ and $[Fe(L)(L^1)]^{2+/3+}$ (L^1 = 1,4,7-trithiacyclononane-1-oxide) [8,9]. The low-spin complex $[Fe(L)_2]^{2+}$ shows a particularly anodic

0022-328X/89/$03.50

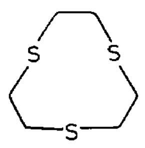

(L)

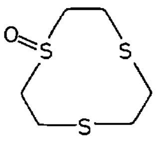

(L¹)

$Fe^{II/III}$ couple ($E_{1/2}$ +0.98 V vs. Fc/Fc$^+$) [8,9]; a similar stabilisation of the d^6 M^{II} centre has also been noted for the Ru^{II} analogue $[Ru(L)_2]^{2+}$ ($E_{1/2}$ +1.41 V vs. Fc/Fc$^+$) [10,11]. We were particularly interested in assessing the stereochemical analogy between carbocyclic moieties such as aryl and cyclopentadienyl ligands and the nine-membered ring tridentate macrocyles; the ability of these ligand systems to bind facially to octahedral metal centres is well documented [1]. We have initiated this study by investigating mixed-sandwich complexes incorporating both carbocyclic and macrocyclic ligands.

Results and discussion

Reaction of $[Fe(C_5H_5)I(CO)_2]$ with one molar equivalent of 1,4,7-trithiacyclononane (L) in refluxing CH_3CN under N_2 affords the complex cation $[Fe(C_5H_5)(L)]^+$. The ^1H NMR spectrum of $[Fe(C_5H_5)(L)]BPh_4$ confirms a Cp : L : BPh_4^- ratio of 1 : 1 : 1, with the proton resonances of the methylene protons giving a complex ABCD pattern centred at 2.45 ppm (Fig. 1). The ^{13}C NMR spectrum of the product showed only two resonances, at δ 35.61 and 74.34 ppm, assigned to the carbon centres of the coordinated thioether and carbocycle, respectively, indicating symmetrical coordination of these moieties to Fe^{II}. The fast atom bombardment mass spectrum of the complex shows a positive ion peak at $M^+ = 301$, with the correct isotopic distribution, corresponding to $[Fe(C_5H_5)(L)]^+$. No other peaks were observed at higher mass units. These data, together with elemental analyses, confirmed the formation of $[Fe(C_5H_5)(L)]^+$.

In order to monitor the stereochemical and conformational features of the complex we undertook a crystallographic study. Single crystals of $[Fe(C_5H_5)(L)]BPh_4$ were grown by diffusion of Et_2O vapour into a solution of the complex in CH_3CN. A view of the cation is shown in Fig. 2. The single crystal X-ray structure confirms

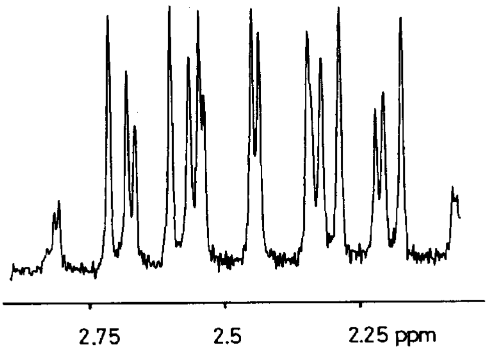

Fig. 1. ^1H NMR spectrum (80 MHz, CD_3NO_2, 293 K) of $[Fe(C_5H_5)(L)]^+$.

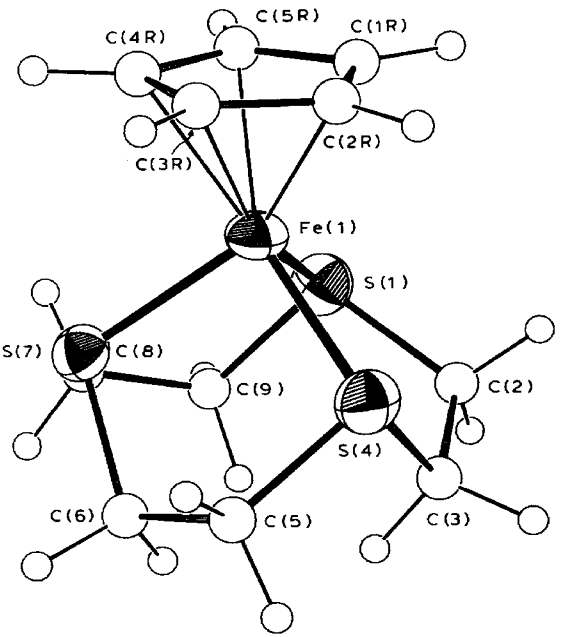

Fig. 2. Single crystal X-ray structure of $[Fe(C_5H_5)(L)]BPh_4$ with numbering scheme adopted. Only one of the two C_5H_5 ring orientations is shown.

the facial coordination of the thioether and carbocyclic ligands to Fe^{II}, Fe–S(1) 2.2100(18), Fe–S(4) 2.2053(19), Fe–S(7) 2.2078(19) Å. Interestingly, the planar cyclopentadienyl moiety is disordered over two equally populated orientations: the two C_5 rings are essentially coplanar but are twisted by 6.18° with respect to each other. This is reminiscent of the disorder observed for the cyclopentadienyl rings in the high temperature solid-state structure of ferrocene [12]. An angle of ca. 3.15° is observed between the S(1)–S(4)–S(7) and C_5 planes in both orientations of the C_5H_5 ligand in the $[Fe(C_5H_5)(L)]^+$ cation.

Cyclic voltammetry of $[Fe(C_5H_5)(L)]PF_6$ shows a reversible one-electron $Fe^{II/III}$ couple at $E_{1/2}$ +0.44 V. vs. Fc/Fc^+, ΔE_p 63 mV. in CH_3CN at platinum electrodes (Fig. 3). Coulometry confirms that the reduction is a one-electron process. The value for this redox process is intermediate between that of $[Fe(L)_2]^{2+}$ [8,9] and ferrocene itself, and reflects the destabilisation of the Fe^{III} oxidation state by (L) relative to the cyclopentadienyl ligand.

Controlled potential electrolysis of $[Fe(C_5H_5)(L)]^+$ at +0.67 V in CH_3CN at a platinum gauze affords the Fe^{III} complex $[Fe(C_5H_5)(L)]^{2+}$, the ESR spectrum of which (measured at 77 K as a CH_3CN glass) shows an anisotropic signal with $g_1 = 2.177$, $g_2 = 2.023$, $g_3 = 1.972$. The UV-vis spectrum of $[Fe(C_5H_5)(L)]^+$ in CH_3CN shows absorption bands at λ_{max} 456 nm (ϵ_{max} 263 M^{-1} cm^{-1}), 371 (351), 266 (9,620) and 222 (18,120). Conversion of Fe^{II} into Fe^{III} can be seen to occur isosbestically (λ_{iso} 290 nm) when an optically transparent thin layer electrode system is used; this is accompanied by a decrease in intensity of the band at 266 nm to ϵ_{max} 7,930 M^{-1} cm^{-1}, and the growth of a shoulder at λ_{max} 312 nm. These results suggest that the absorption band at 266 nm is predominantly a metal-to-ligand charge transfer transition.

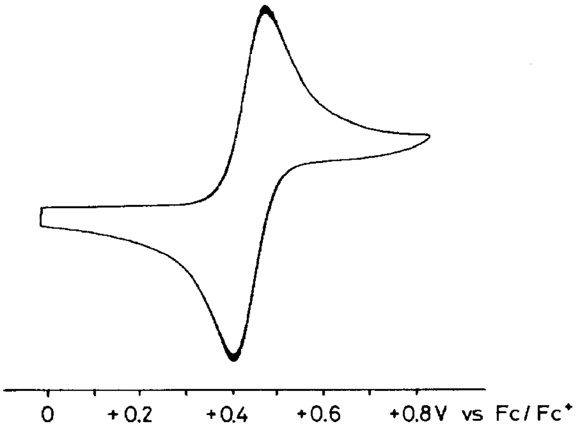

Fig. 3. Cyclic voltammogram of $[Fe(C_5H_5)(L)]PF_6$ in CH_3CN (0.1 *M* $^nBu_4NPF_6$) at platinum electrodes at 273 K.

Current work is aimed at the development of organometallic alkyl and hydrido complexes of Fe^{II} and Ru^{II} with L.

Experimental

Infrared spectra were recorded as Nujol mulls, KBr and CsI discs on a Perkin–Elmer 598 spectrometer over the range 200–4000 cm^{-1}. UV-visible spectra were measured in quartz cells using Perkin–Elmer Lambda 9 and Pye Unicam SP8-400 spectrophotometers. Microanalyses were performed by the Edinburgh University Chemistry Department microanalytical service. ESR spectra were recorded as solids or as frozen glasses down to 77 K using a Bruker ER200D X-band spectrometer. Electrochemical measurements were performed on a Bruker E310 Universal Modular Polarograph. All readings were taken with a three-electrode potentiostatic system in acetonitrile containing 0.1 *M* $^nBu_4NPF_6$ or $^nBu_4BF_4$ as supporting electrolyte. Cyclic voltammetric measurements were carried out with a double platinum electrode and a Ag/AgCl reference electrode. All potentials are quoted versus ferrocene/ferrocinium, Fc/Fc^+. Electron impact mass spectra were recorded on a Kratos MS 902, and FAB spectra on a Kratos MS 50TC spectrometer.

Table 1

Bond lengths (Å) with standard deviations

Fe(1)–S(1)	2.2100(18)	Fe(1)–C(9R)	2.079(11)
Fe(1)–S(4)	2.2053(19)	Fe(1)–C(10R)	2.091(11)
Fe(1)–S(7)	2.2078(19)	S(1)–C(2)	1.826(7)
Fe(1)–C(1R)	2.100(12)	S(1)–C(9)	1.830(6)
Fe(1)–C(2R)	2.112(12)	S(4)–C(3)	1.835(7)
Fe(1)–C(3R)	2.069(12)	S(4)–C(5)	1.832(7)
Fe(1)–C(4R)	2.042(12)	S(7)–C(6)	1.842(7)
Fe(1)–C(5R)	2.007(12)	S(7)–C(8)	1.826(7)
Fe(1)–C(6R)	2.077(11)	C(2)–C(3)	1.498(9)
Fe(1)–C(7R)	2.051(11)	C(5)–C(6)	1.512(10)
Fe(1)–C(8R)	2.024(11)	C(8)–C(9)	1.501(9)

Table 2

Angles (degrees) with standard deviations

S(1)–Fe(1)–S(4)	90.47(7)	Fe(1)–S(7)–C(6)	106.32(23)
S(1)–Fe(1)–S(7)	90.50(7)	Fe(1)–S(7)–C(8)	103.54(22)
S(4)–Fe(1)–S(7)	90.84(7)	C(6)–S(7)–C(8)	100.9(3)
Fe(1)–S(1)–C(2)	103.69(21)	S(1)–C(2)–C(3)	112.5(5)
Fe(1)–S(1)–C(9)	105.97(21)	S(4)–C(3)–C(2)	111.1(5)
C(2)–S(1)–C(9)	99.5(3)	S(4)–C(5)–C(6)	112.9(5)
Fe(1)–S(4)–C(3)	106.06(22)	S(7)–C(6)–C(5)	110.1(5)
Fe(1)–S(4)–C(5)	102.91(24)	S(7)–C(8)–C(9)	112.5(5)
C(3)–S(4)–C(5)	101.1(3)	S(1)–C(9)–C(8)	111.0(4)

Synthesis of [Fe(C_5H_5)(L)]PF_6

Reaction of [Fe(C_5H_5)I$(CO)_2$] (0.067 g, 2.22×10^{-4} mol) with one molar equivalent of L (0.04 g, 2.22×10^{-4} mol) in refluxing CH_3CN under N_2 for 5 h afforded a deep red solution. The solvent was removed in vacuo and the solid product, [Fe(C_5H_5)(L)]I, redissolved in MeOH. Addition of excess of NH_4PF_6 afforded a red precipitate, which was collected and recrystallised from CH_3NO_2 to give [Fe(C_5H_5)(L)]PF_6 (0.065 g, 66%).

Elemental analysis: found: C, 29.7; H, 3.9; S, 22.1. [Fe(C_5H_5)(L)]PF_6 calcd.: C, 29.6; H, 3.8; S, 21.6%. Infrared spectrum (KBr disc): 3120, 1415, 1000, 440 cm^{-1} (C_5H_5); 2960, 2940, 1445, 1415, 1290, 1170, 1120, 955, 910, 670, 410cm^{-1} (L); 840, 555cm^{-1} (PF_6^-). UV-vis spectrum (MeCN): λ_{max} 456 nm (ϵ_{max} 263 M^{-1} cm^{-1}), 371 (351), 266 (9,620), 222 (18,120). ^{13}C NMR spectrum (CD_3CN, 293 K, 50.32 MHz): δ 74.34 (*C*H, C_5H_5), 35.61 ppm (*C*H_2, L). Elemental analysis: found: C, 30.2; H, 4.1. [Fe(C_5H_5)(L)]I calcd.: C, 30.9; H, 4.0%.

Synthesis of [Fe(C_5H_5)(L)]BPh_4

Replacement of NH_4PF_6 by $NaBPh_4$ in the above preparation afforded the corresponding BPh_4^- salt. FAB mass spectrum: found $M^+ = 301$; calculated for [Fe(C_5H_5)(L)]$^+$ $M^+ = 301$ (with correct isotropic distribution). ^1H NMR spectrum (CD_3CN, 298 K, 200 MHz): δ 6.8–7.4 (BPh_4, 20H, m), 4.8 (C_5H_5, 5H, s), 2.45ppm (CH_2, 12H, m).

Table 3

Torsion angles (degrees) of the trithia ligand with standard deviations

C(9)–S(1)–C(2)–C(3)	−69.8(5)
C(3)–S(4)–C(5)–C(6)	−68.2(5)
C(8)–S(7)–C(6)–C(5)	134.5(5)
C(2)–S(1)–C(9)–C(8)	135.6(5)
C(6)–S(7)–C(8)–C(9)	−70.2(5)
S(1)–C(2)–C(3)–S(4)	−44.6(6)
S(4)–C(5)–C(6)–S(7)	−45.0(6)
S(7)–C(8)–C(9)–S(1)	−45.0(6)
C(5)–S(4)–C(3)–C(2)	135.2(5)

X-Ray structure determination of $[Fe(C_5H_5)(L)]BPh_4$

A red crystal (0.46 × 0.46 × 0.35 mm) suitable for X-ray analysis was obtained by isothermal distillation of Et_2O into a solution of the complex in CH_3CN.

Crystal data. $C_{35}H_{37}BFeS_3$, monoclinic, $M = 620.51$, space group $P2_1/c$, with a 15.0461(14), b 10.5866(12), c 19.8032(18) Å, β 100.205(9)°, V 3104.48 Å^3 (from 2θ

Table 4

Fractional coordinates of atoms with standard deviations

	x	y	z	U_{eq}
Fe(1)	0.66556(5)	0.25728(8)	0.06238(4)	0.0387(5)
S(1)	0.80945(10)	0.27927(15)	0.05457(8)	0.0398(9)
S(4)	0.69806(11)	0.28926(17)	0.17408(8)	0.0477(10)
S(7)	0.68452(11)	0.05177(16)	0.07753(9)	0.0458(10)
C(2)	0.8588(4)	0.3555(6)	0.1352(3)	0.048(4)
C(3)	0.8213(4)	0.3050(7)	0.1951(3)	0.053(4)
C(5)	0.6819(5)	0.1327(7)	0.2094(4)	0.062(5)
C(6)	0.7183(5)	0.0272(6)	0.1706(3)	0.055(5)
C(8)	0.7910(4)	0.0207(6)	0.0484(4)	0.052(5)
C(9)	0.8598(4)	0.1222(6)	0.0698(3)	0.044(4)
C(1R)	0.5294(8)	0.2304(11)	0.0182(7)	0.049(5)
C(2R)	0.5800(8)	0.2269(11)	−0.0329(7)	0.042(5)
C(3R)	0.6247(8)	0.3399(11)	−0.0327(7)	0.045(5)
C(4R)	0.6008(8)	0.4139(11)	0.0180(7)	0.065(5)
C(5R)	0.5453(8)	0.3442(11)	0.0517(7)	0.075(9)
C(6R)	0.6311(6)	0.4068(12)	−0.0051(6)	0.049(4)
C(7R)	0.6017(6)	0.2948(12)	−0.0359(6)	0.056(4)
C(8R)	0.5431(6)	0.2406(12)	0.0014(6)	0.069(5)
C(9R)	0.5335(6)	0.3219(12)	0.0538(6)	0.047(6)
C(10R)	0.5892(6)	0.4235(12)	0.0504(5)	0.049(4)
B(1)	0.7788(4)	0.7415(7)	0.3565(3)	0.032(4)
C(1′)	0.78237(25)	0.7785(4)	0.43962(14)	0.037(4)
C(2′)	0.70570(25)	0.7574(4)	0.46866(14)	0.043(4)
C(3′)	0.70930(25)	0.7755(4)	0.53888(14)	0.050(4)
C(4′)	0.78959(25)	0.8145(4)	0.58006(14)	0.059(5)
C(5′)	0.86626(25)	0.8356(4)	0.55102(14)	0.054(5)
C(6′)	0.86265(25)	0.8175(4)	0.48081(14)	0.046(4)
C(7′)	0.80405(25)	0.5869(3)	0.36145(19)	0.035(4)
C(8′)	0.73732(25)	0.4940(3)	0.34974(19)	0.043(4)
C(9′)	0.76012(25)	0.3675(3)	0.36262(19)	0.059(5)
C(10′)	0.84964(25)	0.3338(3)	0.38723(19)	0.066(5)
C(11′)	0.91637(25)	0.4267(3)	0.39894(19)	0.060(5)
C(12′)	0.89357(25)	0.5532(3)	0.38606(19)	0.044(4)
C(13′)	0.85276(23)	0.8251(3)	0.32009(17)	0.032(4)
C(14′)	0.88915(23)	0.7713(3)	0.26673(17)	0.036(4)
C(15′)	0.94320(23)	0.8436(3)	0.23119(17)	0.046(4)
C(16′)	0.96086(23)	0.9698(3)	0.24899(17)	0.044(4)
C(17′)	0.92447(23)	1.0236(3)	0.30235(17)	0.044(4)
C(18′)	0.87042(23)	0.9513(3)	0.33789(17)	0.041(4)
C(19′)	0.67958(21)	0.7741(4)	0.30644(17)	0.037(4)
C(20′)	0.65231(21)	0.7067(4)	0.24580(17)	0.047(4)
C(21′)	0.57296(21)	0.7399(4)	0.20155(17)	0.060(5)
C(22′)	0.52089(21)	0.8406(4)	0.21795(17)	0.067(6)
C(23′)	0.54817(21)	0.9081(4)	0.27859(17)	0.061(5)
C(24′)	0.62752(21)	0.8748(4)	0.32283(17)	0.048(4)

values of 36 reflections measured at $\pm\omega$ (2θ 24–26°, $\bar{\lambda} = 0.71073$ Å)], D_c 1.327 g cm^{-3}, $Z = 4$; $F(000) = 1304$, μ 6.70 cm^{-1}.

Data collection and processing. Stoe–Siemens AED2 four-circle diffractometer, Mo-K_α X-radiation, ω–2θ scans with ω scan width $(0.80 + 0.347 \tan\theta)°$, 4138 reflections measured to 2θ 45°, giving 2519 with $F \geqslant 6\sigma(F)$. No significant crystal decay, no absorption correction.

Structure analysis and refinement. The Fe and S atoms were located by direct methods [13] followed by iterative least-squares refinement and difference Fourier synthesis [14] to locate all other non-H atoms. Anisotropic thermal parameters were refined for all Fe, S, B and C atoms except those of the disordered cyclopentadienyl ring: two orientations of this ring were modelled successfully by refinement as planar rigid groups with C–C distances of 1.373 Å and C–C–C angles of 108°. H atoms on the macrocycle, on the BPh_4^- counter-ion and on both orientations of the cyclopentadienyl ring were included in fixed, calculated positions [14]. The weighting scheme $w^{-1} = \sigma^2(F) + 0.00058F^2$ gave satisfactory analyses. At convergence, $R, R_w = 0.0484$ and 0.0598 respectively for 291 parameters, $S = 1.166$. The maximum and minimum residues in the final ΔF syntheses were 0.39 and -0.38 eÅ^{-3} respectively. Illustrations were prepared using ORTEP [15], molecular geometry calculations utilised CALC [16], and scattering factor data were taken from ref. 17. Bond lengths, angles, torsion angles and fractional coordinates are given in Tables 1–4. Lists of thermal parameters, hydrogen atom coordinates, and observed and calculated structure factors are available from the author.

Acknowledgements

We thank SERC for support.

References

1 M. Schröder, Pure Appl. Chem., 60 (1988) 517 and ref. therein.

2 H.-J. Küppers, A. Neves, C. Pomp, D. Ventur, K. Wieghardt, B. Nuber and J. Weiss, Inorg. Chem., 25 (1986) 2400.

3 M.T. Ashby and D.L. Lichtenberger, Inorg. Chem., 24 (1985) 636.

4 R.S. Glass, W.N. Setzer, C.A. Ogle and G.S. Wilson, Inorg. Chem., 22 (1983) 266; G.S. Wilson, D.D. Swanson and R.S. Glass, ibid., 25 (1986) 3827.

5 E.W. Abel, P.D. Beer, I. Moss, K.G. Orrell, V. Šik, P.A. Bates and M.B. Hursthouse, J. Chem. Soc., Chem. Commun., (1987) 978; E.W. Abel, P.D. Beer, I. Moss, K.G. Orrell, V. Šik, P.A. Bates and M.B. Hursthouse, J. Organomet. Chem., 341 (1988) 559.

6 D. Sellmann and P. Frank, Angew. Chem., 98 (1986) 1115; Angew. Chem. Int. Ed. Engl., 25 (1986) 1107.

7 J.R. Hartman and S.R. Cooper, J. Am. Chem. Soc., 108 (1986) 1202; J.R. Hartman, and S.R. Cooper, ibid., 108 (1986) 1208.

8 K. Wieghardt, H.-J. Küppers and J. Weiss, Inorg. Chem., 24 (1985) 3067.

9 H.-J. Küppers, K. Wieghardt, B. Nuber, J. Weiss, E. Bill and A.X. Trautwein, Inorg. Chem., 26 (1987) 3762.

10 M.N. Bell, A.J. Blake, H.-J. Küppers, M. Schröder and K. Wieghardt, Angew. Chem., 99 (1987) 253; Angew. Chem. Int. Ed. Engl., 26 (1987) 250.

11 S.C. Rawle, T.J. Sewell and S.R. Cooper, J. Chem. Soc., Chem. Commun., (1987) 308; S.C. Rawle, T.J. Sewell and S.R. Cooper, Inorg. Chem., 26 (1987) 3769.

12 P. Seiler and J. Dunitz, Acta Crystallogr., B, 35 (1979) 1068. For discussion see: E.A.V. Ebsworth, D.W.H. Rankin and S. Cradock (Eds.), Structural Methods in Inorganic Chemistry, p. 375–378, Blackwell Scientific Publications, Oxford, 1987.

13 SHELX86, Program for Crystal Structure Solution, G.M. Sheldrick, University of Göttingen, 1986.
14 SHELX76, Program for Crystal Structure Determination, G.M. Sheldrick, University of Cambridge, 1976.
15 ORTEPII, interactive version. P.D. Mallinson and K.W. Muir, J. Appl. Cryst., 18 (1985) 51.
16 CALC, Fortran77 version. R.O. Gould and P. Taylor, University of Edinburgh, 1985.
17 D.T. Cromer and J.L. Mann, Acta Crystallogr., A, 24 (1968) 321.